Citation: CPT Pharmacometrics Syst. Pharmacol. (2015) 4, 585–594; doi:10.1002/psp4.12010


ORIGINAL ARTICLE

# Quantitative Systems Pharmacology Approaches Applied to Microphysiological Systems (MPS): Data Interpretation and Multi-MPS Integration

J Yu[1], NA Cilfone[1], EM Large[2], U Sarkar[1], JS Wishnok[1], SR Tannenbaum[1,3], DJ Hughes[2], DA Lauffenburger[1], LG Griffith[1,4], CL Stokes[5] and M Cirit[1]*

**Our goal in developing Microphysiological Systems (MPS) technology is to provide an improved approach for more predictive preclinical drug discovery via a highly integrated experimental/computational paradigm. Success will require quantitative characterization of MPSs and mechanistic analysis of experimental findings sufficient to translate resulting insights from *in vitro* to *in vivo*. We describe herein a systems pharmacology approach to MPS development and utilization that incorporates more mechanistic detail than traditional pharmacokinetic/pharmacodynamic (PK/PD) models. A series of studies illustrates diverse facets of our approach. First, we demonstrate two case studies: a PK data analysis and an inflammation response—focused on a single MPS, the liver/immune MPS. Building on the single MPS modeling, a theoretical investigation of a four-MPS interactome then provides a quantitative way to consider several pharmacological concepts such as absorption, distribution, metabolism, and excretion in the design of multi-MPS interactome operation and experiments.**
*CPT Pharmacometrics Syst. Pharmacol.* (2015) **4**, 585–594; doi:10.1002/psp4.12010; published online on 5 October 2015.

## Study Highlights

WHAT IS THE CURRENT KNOWLEDGE ON THE TOPIC? ☑ Microphysiological Systems (MPS) development is an emerging technology for predictive preclinical drug discovery approaches. Even though advanced *in vitro* MPS models have been recently developed, quantitative understanding from such systems is still limited. • WHAT QUESTION DID THIS STUDY ADDRESS? ☑ How systems pharmacology approach can be used to advance experimental design and data interpretation in microphysiological systems, and the development of a multi-MPS platform. • WHAT THIS STUDY ADDS TO OUR KNOWLEDGE ☑ We provide a methodology for this emerging field using systems biology and systems pharmacology principles. The use of model-based data interpretation, experimental design, and system integration is essential for such complex systems. Moreover, in comparison to traditional PK models, systems pharmacology models provide more mechanistic knowledge of biological and pharmacological processes. • HOW THIS MIGHT CHANGE CLINICAL PHARMACOLOGY AND THERAPEUTICS ☑ Integration of system pharmacology and advances in tissue engineering (microphysiological systems) may provide improved translation of preclinical findings to clinical outcomes.

Lack of efficacy and unpredicted toxicity continue to cause high failure rates for drug candidates in clinical trials.[1–3] The *in vitro* cell culture models and *in vivo* animal models commonly used in preclinical studies provide limited information relevant to human physiology.[4,5] Therefore, new approaches that are more easily translated to and predictive of human clinical outcomes are desirable.[6] A major effort to improve preclinical models is the development of "Microphysiological Systems" (MPSs) using engineered human tissues that capture more physiological complexity than standard cell cultures.[7] An MPS typically contains cocultures of human primary cells, 3D microenvironments, and some degree of physiological mechanical and chemical stimulation. Integration of multiple MPS constructs on a single platform potentially enables pharmacologic and toxicological studies of interacting human tissues and organ systems, provided appropriate computational models can be used to translate from *in vitro* to *in vivo*.

Seminal work by Shuler and colleagues beginning in the early 1990s demonstrated that pharmacological communication between several organ system mimics could occur in a multicompartmental bioreactor system.[8] These interacting organ systems could be miniaturized onto a 1-inch by 1-inch silicon chip[9] and interfaced with instrumentation to measure physiological parameters.[10] A parallel shift in emphasis in the field of tissue engineering, from regenerative medicine applications to *in vitro* models,[11] has resulted in numerous new complex models of liver, lung, gut, skin, muscle, blood vessels, and other tissues.[12–18] A substantial push to further improve 3D models and integrate them to improve translation of preclinical pharmacokinetics, efficacy, and toxicology results from lab to clinic arose recently with establishment in 2012 of the Microphysiological Systems program by the United States Defense Advanced Research Projects Agency, National Institutes of Health, and Food and Drug Administration.[19]

[1]Department of Biological Engineering, Massachusetts Institute of Technology, Cambridge, Massachusetts, USA; [2]CN Bio Innovations, Welwyn Garden City, UK; [3]Department of Chemistry, Massachusetts Institute of Technology, Cambridge, Massachusetts, USA; [4]Center of Gynepathology, Massachusetts Institute of Technology, Cambridge, Massachusetts, USA; [5]Stokes Consulting, Redwood City, California, USA. *Correspondence: M Cirit (mcirit@mit.edu)
Received 30 April 2015; accepted 9 July 2015; published online on 5 October 2015. doi:10.1002/psp4.12010

As the complexity of *in vitro* systems increases, experimental design and data interpretation become more challenging. Successful use of single and multi-MPS platforms for pharmacologic studies requires systematic characterization of the relationships between drug exposure, MPS biological responses, and MPS–MPS interactions. While a variety of pharmacokinetic/pharmacodynamic (PK/PD) models are used to characterize relationships between drug kinetics and biological effects in *in vivo* models, the scope of existing models is too limited for design of *in vitro* systems and interpretation of data emerging from their operation.[20,21] Instead, computational models with greater mechanistic detail capturing interrelated physical (e.g., inter-MPS flowrates) and biological (e.g., cytokine/growth factor/hormone production and release) dynamics will be needed to rationally design functional MPSs, select experimental conditions, analyze and predict related human outcomes. Moving from traditional empirical PK/PD models towards more mechanistic models such as physiologically based PK (PBPK) models and systems pharmacology models will not only provide greater power for predicting clinical outcomes but will also offer more insight into the biological systems of interest.[6]

Herein, we use systems pharmacology models for MPS experimental design, data interpretation, and multi-MPS platform integration. Data acquisition from the multi-MPS platforms comprises measurements of soluble entities: drugs and cell-produced molecules. Hence, our models track exogenously administered soluble molecules (drugs, medium components), modified molecules of exogenous entities (metabolites), endogenously secreted biomolecules (e.g., albumin, bile acids), and serological disease and PD response markers (e.g., cytokines and growth factors), as needed for a particular application. These models include several pharmacological and physiological processes such as absorption through epithelial barriers, molecular distribution between MPSs, and drug metabolism, excretion, and protein binding. We first use these models to analyze drug metabolism and disease response marker measurements from a single MPS, the micro-perfused liver/immune MPS,[22,23] demonstrating the use of systems pharmacology models for interpreting experimental results and guiding experimental design. Building from such models of single MPSs, the design and operational principles of a four-MPS interactome are then theoretically investigated with the systems pharmacology approach.

## MATERIALS AND METHODS

### Liver/immune MPS experimental studies

The liver/immune MPS comprises a 3D coculture of human hepatocytes and Kupffer cells, as previously described in studies of drug metabolism, toxicity, and aspects of the liver immune response.[13,22–24] This MPS was used herein to study the PK of hydrocortisone (HC) as well as the liver inflammatory response to lipopolysaccharides (LPSs). Details regarding the culture of liver/immune MPS, HC, and cytokine quantification are in the **Supplementary Material**.

### Modeling and simulation

All modeling and simulation were performed in MATLAB (R2014a, MathWorks, Natick, MA). MATLAB's Genetic Algorithm in Optimization Toolbox was used for parameter estimation. MATLAB's Statistics Toolbox was used to perform the two-way mixed design analysis of variance (ANOVA). Global sensitivity analysis was performed using Latin Hypercube Sampling (LHS) and Partial Rank Correlation Coefficient (PRCC).

The traditional PK and mechanistic PK models for HC and the model of inflammatory response to LPS stimulation are detailed in the **Supplementary Material.**

A theoretical four-MPS interactome consisting of liver, kidney, gut, and hypothetical PD MPS was computationally modeled. The model includes oral drug absorption through the gut epithelial barrier, plasma protein binding, unbound drug metabolism in the liver MPS, drug excretion in the kidney MPS, and drug transport between MPSs. The mixing chamber is analogous to a blood compartment and allows for the equivalent of intravenous drug administration and media sampling. The inter-MPS flow rates are scaled based on *in vivo* blood flow partitioning. Percentages of adult human blood flow rates to kidney, portal vein, and hepatic artery are 19%, 19%, and 6% of the cardiac output, respectively.[25] Thus, for this study the flow rates to kidney, gut, hepatic artery, and the PD MPS in the four-MPS interactome were specified as 40%, 40%, 10%, and 10% of the mixing chamber output ($Q_{mixing}$), with the last being appropriate to a highly vascularized organ like skin. This split would be adjusted appropriately for any specified PD MPS. Details of this model and the global sensitivity analysis are in the **Supplementary Material**.[26]

## RESULTS

### Mechanistic pharmacokinetics of hydrocortisone in liver/immune MPS

We first compare how a traditional PK model and a mechanistic model provide different insights from *in vitro* systems. Specifically, we study the effects of different concentrations of human serum albumin (HSA) and cell culture periods on HC PK in the liver/immune MPS. In humans, HC binds to HSA and corticosteroid binding globulin (CBG) in blood, leaving a small fraction unbound[27]; importantly, only the unbound form functions biologically and can be metabolized.[28,29]

In our experiments, HC concentration was measured in the presence of low (1.25 mg/mL) and high (25 mg/mL) HSA concentrations over 48 hours starting at culture day 3 or day 5 and the resulting PK was analyzed. Total HC metabolism was modeled with a traditional PK model that characterizes the disappearance of total HC as a single metabolizable species (**Supplementary Figure 1**). For comparison, HC metabolism was analyzed with a more mechanistic model that accounted for HC binding to HSA, in which only unbound HC was metabolized by hepatocytes. Equilibrium binding simulations (**Supplementary Figure 2**), using published kinetic parameters[30–32] for binding of HC and HSA, predicted that 5% and 53% of HC was initially bound to HSA at 1.25 mg/mL and 25 mg/mL HSA,

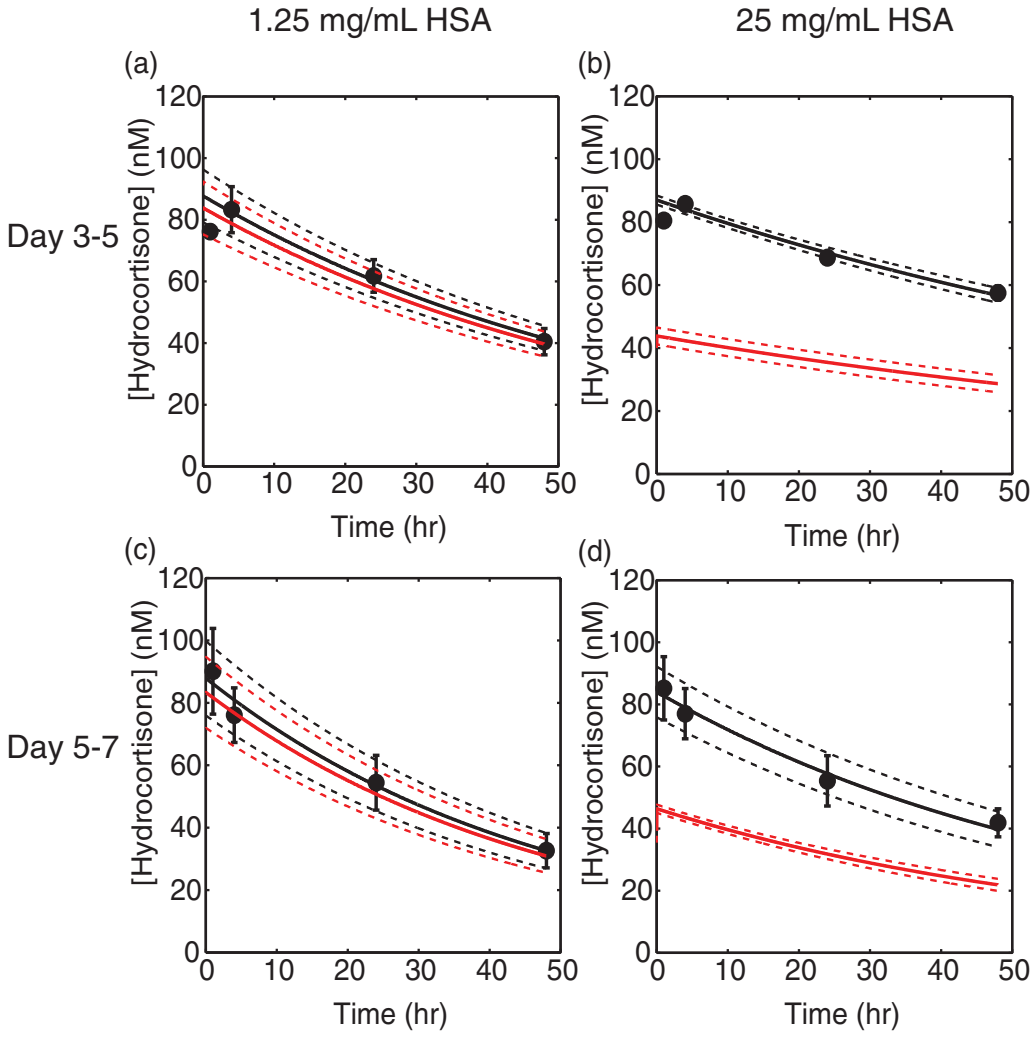


**Figure 1** PK modeling of HC metabolism in the liver/immune MPS. HC PK data measured from the liver/immune MPS experiment on culture day 3 to day 5 (**a,b**) and day 5 to day 7 (**c,d**) for low (**a,c**) and high (**b,d**) HSA concentrations were fitted to the mechanistic model. Black lines correspond to total HC concentrations and red lines to free HC. Error bars and dashed lines represent SEM of measured data and fitted curves, respectively ($n = 3$).

respectively. The metabolism rate constants of total HC ($k_{metabolism,total}$) in the traditional PK model and free (unbound) HC ($k_{metabolism,unbound}$) in the mechanistic PK model were calculated by fitting the experimental HC kinetic profiles (**Figure 1, Supplementary Figure 1,** and **Table 1**).

We investigated whether the calculated PK parameters from each model were dependent on either HSA concentration or culture period using two-way mixed design ANOVA (**Supplementary Table 1**). Data analysis by the traditional PK model (i.e., the binding to HSA is not accounted for) revealed that the apparent total HC metabolism rate constant ($k_{metabolism,total}$) depends on both the cell culture period (days 3–5 vs. days 5–7, $P = 0.0012$) and on the HSA concentration ($P = 0.039$). In comparison, using the mechanistic PK model the metabolic rate constant derived for unbound HC ($k_{metabolism,unbound}$) is unaffected by HSA concentration ($P = 0.22$), although it was still dependent on cell culture period ($P = 0.0082$). No significant interaction

**Table 1** HC pharmacokinetic parameters measured from the liver/immune MPS

| Traditional (non-mechanistic) PK model $k_{metabolism,total}$ (mean ± SEM, $\times 10^{-2}$/hr) | | | Mechanistic PK model $k_{metabolism,unbound}$ (mean ± SEM, $\times 10^{-2}$/hr) | | |
|---|---|---|---|---|---|
| | **Low HSA** | **High HSA** | | **Low HSA** | **High HSA** |
| Day 3-5 | 1.6 ± 0.1 | 0.9 ± 0.1 | Day 3-5 | 1.6 ± 0.1 | 1.8 ± 0.2 |
| Day 5-7 | 2.1 ± 0.2 | 1.6 ± 0.2 | Day 5-7 | 2.2 ± 0.2 | 2.8 ± 0.3 |

Total HC metabolism rates ($k_{metabolism,total}$) were obtained with the traditional one-compartment PK model. Unbound HC metabolism rates ($k_{metabolism,unbound}$) were obtained with the mechanistic model. Data and curve fits are shown in **Figures 1** and **S1**.

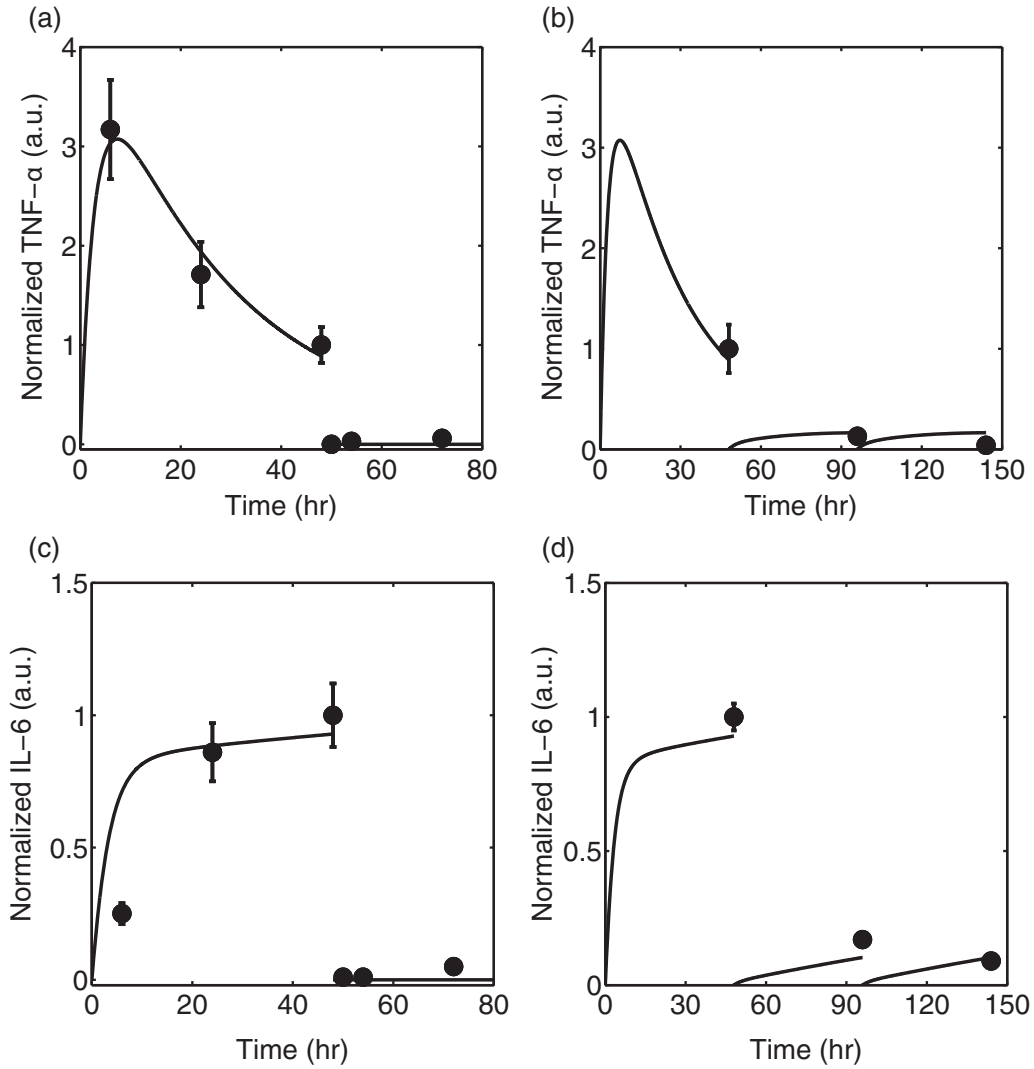


**Figure 2** Modeling of the inflammatory responses in the liver/immune MPS. Net production of TNF-α appears transient (**a**) while that of IL-6 is sustained (**c**). Subsequent doses of LPS fail to stimulate TNF-α (**b**) and IL-6 (**d**) secretion. The discontinuity at the 48-hour time-point reflects a medium change. Symbols and error bars are measured data and SEM ($n = 3$). Solid lines are model fitted curves.

between HSA concentration and cell culture period was found in either model (**Supplementary Table 1**). Considering the effect of HSA concentration alone, the traditional PK model resulted in a nonconstant $k_{metabolism,total}$ as HSA concentration varies. In contrast, the mechanistic PK analysis had a constant value of $k_{metabolism,unbound}$ as HSA concentration (and therefore initial HC bound/unbound ratio) varies, suggesting that it can be used to study drug PK at different plasma protein concentrations, e.g., *in vivo* studies. Even so, the value of $k_{metabolism,unbound}$ was sensitive to MPS culture period. This suggests that MPS function over time must be better understood to select appropriate MPS experimental conditions that will potentially be translatable to *in vivo* human PK.

### Semimechanistic analysis of inflammatory response biomarkers in the liver/immune MPS

Next we investigated the inflammatory response of the liver/immune MPS to stimulation with repeated doses of LPS using a semimechanistic model for production of two inflammatory cytokines. LPS, secreted by Gram-negative bacteria, induces cytokine release via binding of Toll-like receptor 4 (TLR4) on Kupffer and other immune system cells.[33–36]

An initial dose of LPS (1 μg/ml) induced a strong inflammatory response in the liver/immune MPS, with a transient increase of secreted tumor necrosis factor-α (TNF-α) and more sustained increase of interleukin-6 (IL-6). TNF-α and IL-6 secretion was diminished after the removal of the inflammatory stimulus (LPS) after 48 hours with complete media change (**Figure 2a,c**). The repeated LPS dosing every 48 hours induced inflammatory response only after the first dose and failed to stimulate a significant response for the subsequent doses (**Figure 2b,d**).

A semimechanistic model including LPS-binding of TLR4, LPS-TLR4 complex internalization, TLR4 recycling, and TNF-α and IL-6 production by Kupffer cells was used to investigate possible mechanisms underlying these

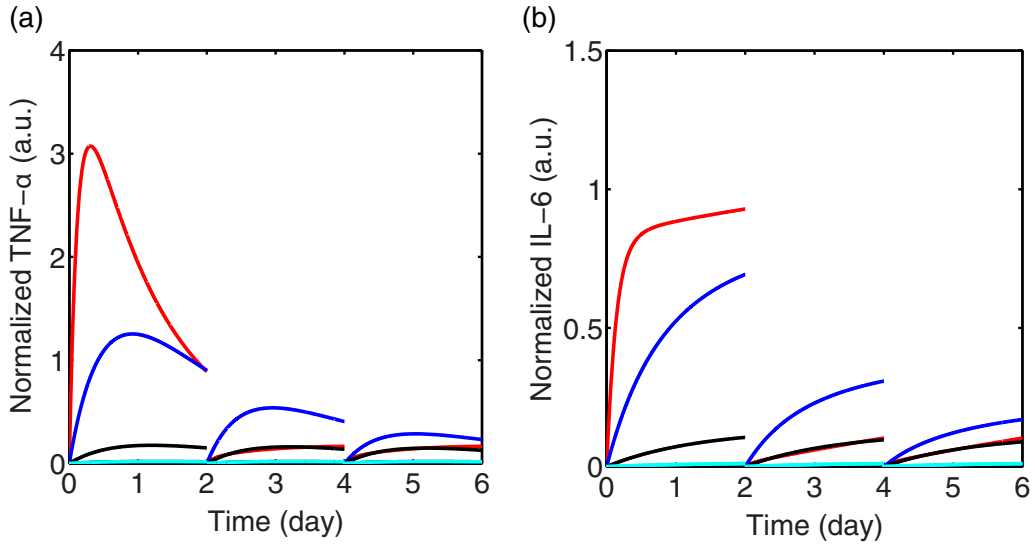


**Figure 3** A semimechanistic model of LPS-TLR4 binding, internalization, and trafficking predicts muting of inflammatory response on repeated dosing. Simulated liver/immune MPS inflammatory responses to LPS doses of 1 μg/ml (red), 0.1 μg/ml (blue), 0.01 μg/ml (black), and 0.001 μg/ml (cyan). LPS was added to the liver/immune MPS as a bolus dose at time 0 and again at the time of subsequent medium changes (48 and 96 hours), and the resulting temporal evolution of the concentrations of TNF-α (**a**) and IL-6 (**b**) were simulated.

observations (**Supplementary Figure 3**). The model recapitulated the experimental observations, including desensitization to subsequent doses of LPS (**Figure 2** and **Supplementary Figure 4**). The model predicted that the loss of cytokine response to a second high LPS dose (1 μg/ml) was consistent with the saturation and internalization of TLR4 receptors on the cell surface, coupled with a relatively slow recycling rate of LPS-TLR4 complexes. In comparison, simulations predicted that a more moderate level of LPS (0.1 μg/mL) could induce a smaller but more sustained response over multiple doses, while even lower levels of LPS (<0.01 μg/mL) failed to elicit a substantial inflammatory response (**Figure 3**). With further quantification and characterization of the system, such simulations using this data-driven modeling paradigm will be critical for guiding experimental design, studying disease biology, and could similarly be used for pharmaco- and toxicodynamic studies.

### Systems pharmacology-guided interactome design

In this section we focus on model-guided multi-MPS interactome development, combining mechanistic modeling of individual MPSs, as developed in the last two sections, with PBPK modeling principles for the interactome. A four-MPS interactome consisting of gut, liver, kidney, and PD MPSs plus a mixing chamber was the focus because of its relevance for comprehensive PK and PD studies (**Figure 4**). The PD MPS is a placeholder for any MPS in which drug PD is of interest, for instance, skin, cardiac muscle, cartilage, or brain.

We used our four-MPS systems pharmacology model to investigate how biological and operational parameters govern the transport and fate of endogenous and exogenous molecules in the four-MPS interactome. First, we considered the distribution and fate of a molecule produced endogenously by the liver MPS (e.g., bile acids, albumin, or

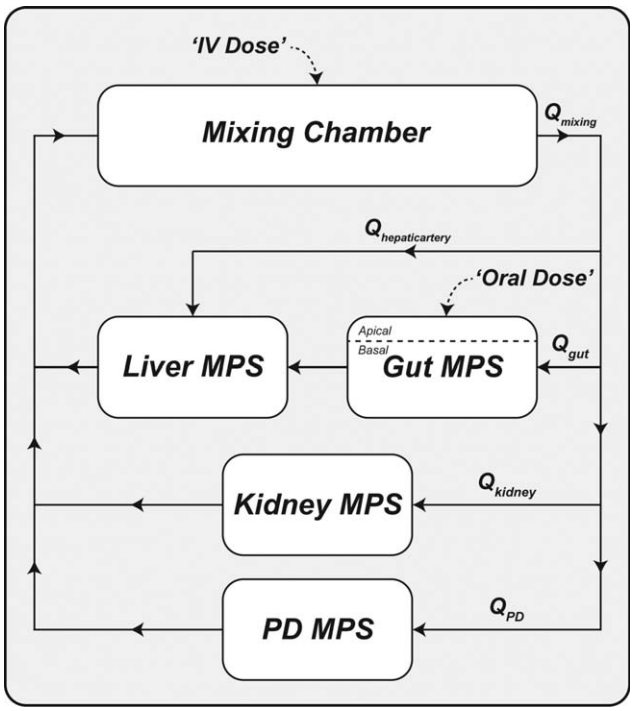


**Figure 4** Model structure for the four-MPS interactome (Gut MPS, Liver MPS, Kidney MPS, PD MPS, and mixing chamber). In the four-MPS model, $Q_{mixing}$ is the sum of $Q_{hepatic\ artery}$, $Q_{gut}$, $Q_{kidney}$, and $Q_{PD}$.

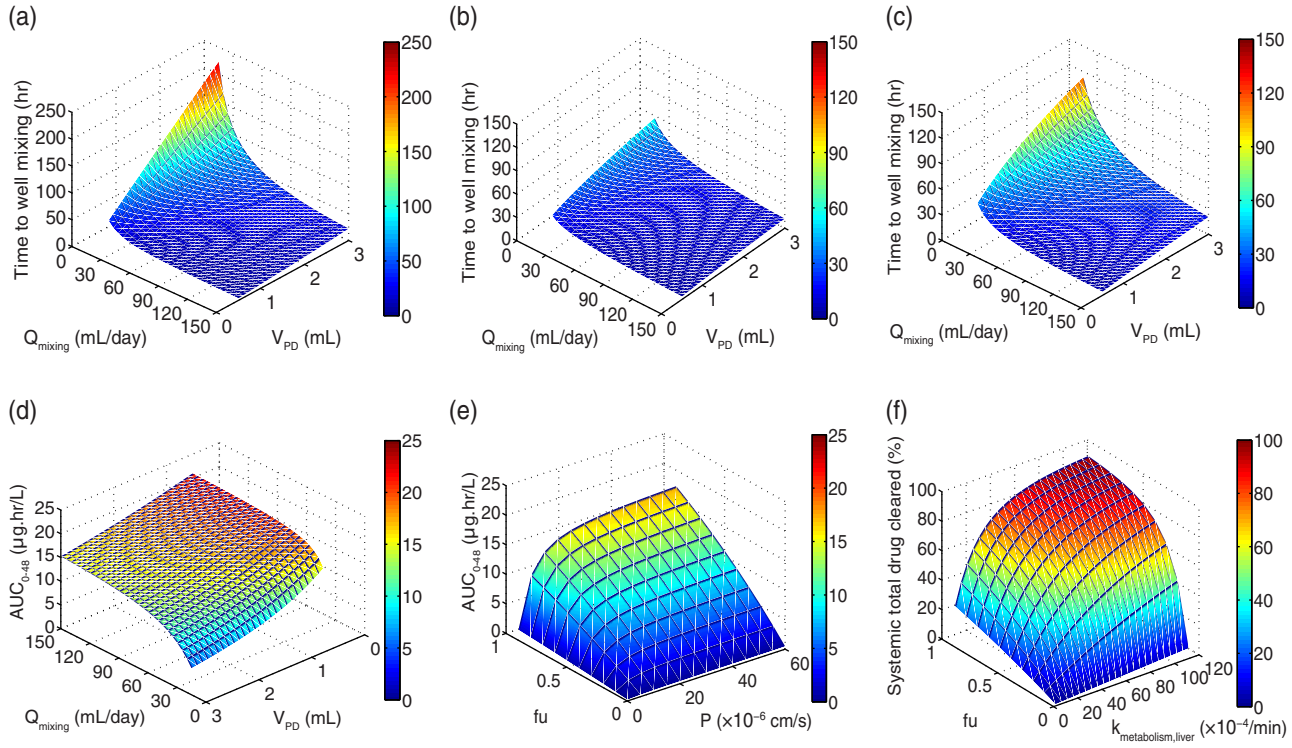


**Figure 5** Simulations of the four-MPS interactome. (**a**) $t_{mixing,80}$ for an endogenously produced molecule as a function of $Q_{mixing}$ and $V_{PD}$. (**b,c**) $t_{mixing,80}$ for a drug administered to the apical side of the gut ("oral administration"), as a function of $Q_{mixing}$ and $V_{PD}$, for cases of high intestinal drug permeability, ((**b**), $P = 20 \times 10^{-6}$ cm/s) and low intestinal drug permeability ((**c**), $P = 1 \times 10^{-6}$ cm/s). (**d**) $AUC_{0\text{-}48,PD}$ for unbound drug as a function of $Q_{mixing}$ and $V_{PD}$ for orally administered drug. (**e**) $AUC_{0\text{-}48,PD}$ for unbound drug as function of fraction of drug unbound ($fu$) and $P$ for orally administered drug. (**f**) Systemic total drug cleared percentage at 48 hours following oral administration of drug as a function of fraction of drug unbound ($fu$) and hepatic metabolism rate constant ($k_{metabolism,liver}$).

cytokines). We assumed a constant production rate in the liver MPS and no elimination in any MPS. From a design and operational view, an important consideration is how quickly molecules will become "well-mixed" throughout the system. The time required for the concentration of a chemical entity in the PD MPS to reach 80% of that in the mixing chamber ($t_{mixing,80}$) was used as the output function in global sensitivity analysis to evaluate the effects of parameters on concentration uniformity in the system.[26] The analysis indicated that $t_{mixing,80}$ of an endogenously produced molecule strongly depended on mixing chamber outlet flow rate ($Q_{mixing}$) and PD MPS media volume ($V_{PD}$), while other model parameters had minimal effects (**Supplementary Table 2**). **Figure 5a** shows that as $V_{PD}$ increases, $t_{mixing,80}$ also increases proportionally, as expected for dilution due to added volume. In contrast, the effect of $Q_{mixing}$ on $t_{mixing,80}$ is nonlinear: increasing inter-MPS flow by raising $Q_{mixing}$ from 0 to about 30–60 ml/day (depending on $V_{PD}$) strongly decreases $t_{mixing,80}$, while further increases have much less effect. Hence a $Q_{mixing}$ of about 30–60 ml/day (given the other parameter values specified) is the highest needed if uniform concentration in the system is the primary interest.

To guide studies of drug absorption, distribution, metabolism, and excretion in the four-MPS interactome, we investigated the effect of operational and biological parameters on several measures important for PD. Specifically, the time for the PD MPS and mixing chamber to become well-mixed following drug administration, drug exposure, and the elimination of total drug in the platform. An oral drug was assumed to be administered as a bolus to the gut MPS apical side, absorbed to the basal side, and distributed to the other MPSs (**Figure 4**). It can be metabolized by the liver MPS and excreted by the kidney MPS only when unbound. Sensitivity analysis for $t_{mixing,80}$ relating uniformity of PD MPS and mixing chamber indicates that $Q_{mixing}$, $V_{PD}$, and drug intestinal permeability coefficient ($P$) are the primary drivers (**Supplementary Table 3**). The effects of a range of $Q_{mixing}$ and $V_{PD}$ for high ($20 \times 10^{-6}$ cm/s) and low ($1 \times 10^{-6}$ cm/s) permeability coefficients are illustrated in **Figure 5b,c,** respectively. Faster $Q_{mixing}$ and smaller $V_{PD}$ result in shorter times to reach uniform concentration in the system regardless of permeability. Low permeability drugs take longer to reach uniformity than high permeability drugs, however, for any $Q_{mixing}$ and $V_{PD}$.

Pharmacodynamic effects of a drug depend not only on its concentration but also on exposure of tissue to bioavailable (unbound) drug. Hence, we examined area under the curve of unbound drug from 0 to 48 hours ($AUC_{0\text{-}48}$) in the PD MPS following administration to the apical side of the gut MPS. Sensitivity analysis of $AUC_{0\text{-}48}$ in the PD MPS showed that the fraction of unbound drug ($fu$) had the strongest modulating effect, while $V_{PD}$, $Q_{mixing}$, and $P$ had modest effects (**Supplementary Table 3**). **Figure 5d**

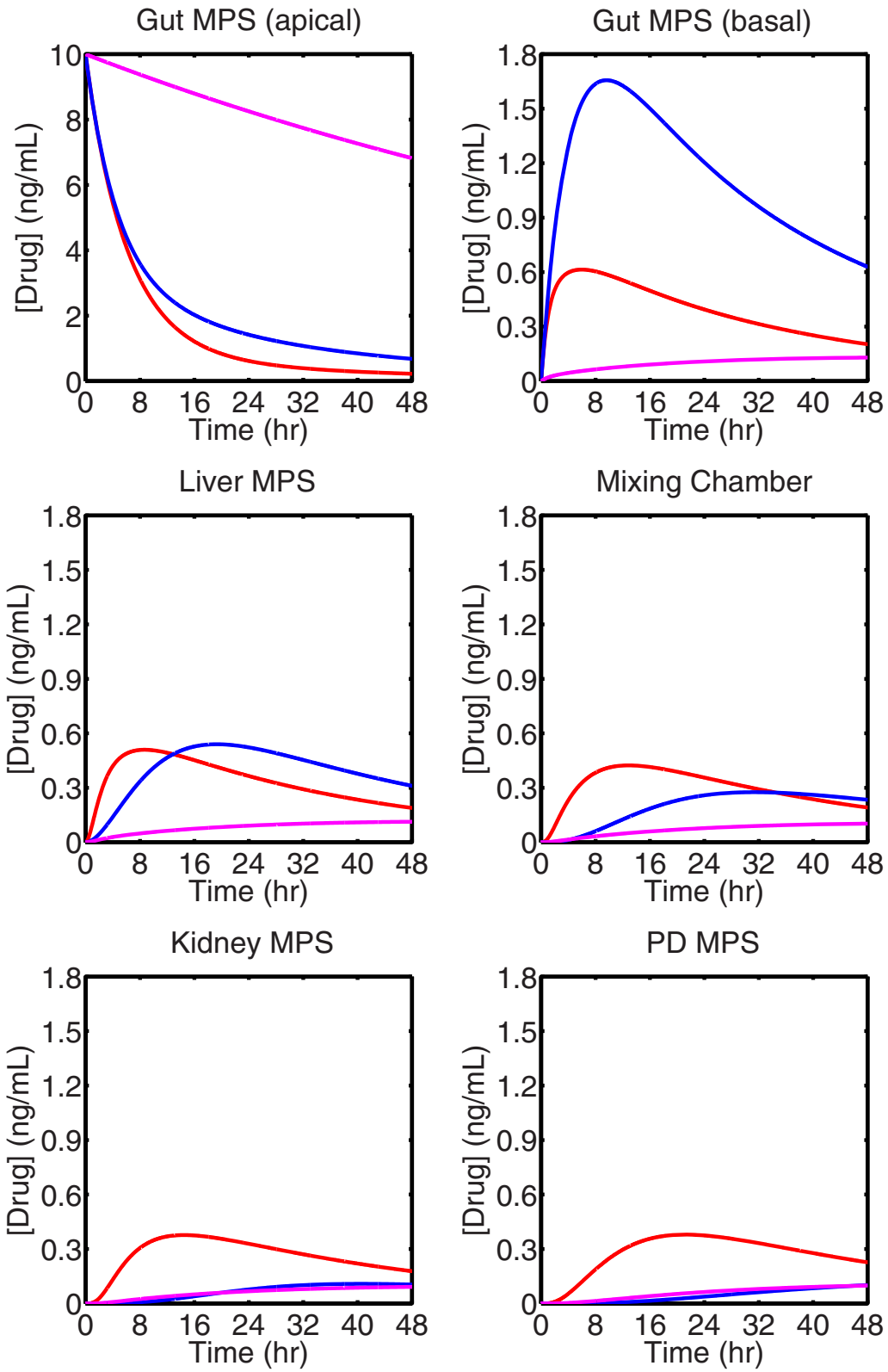


**Figure 6** Simulations of drug concentration in each MPS plus mixing chamber of the four-MPS interactome for the oral drug administration scenario and several combinations of parameter values; (red) high intestinal permeability coefficient $P$ ($20 \times 10^{-6}$ cm/s) with high $Q_{mixing}$ (60 mL/day); (blue) high $P$ ($20 \times 10^{-6}$ cm/s) with low $Q_{mixing}$ (5 mL/day); (magenta) low $P$ ($P = 1 \times 10^{-6}$ cm/s) with high $Q_{mixing}$ (60 mL/day).

shows that exposure to unbound drug in the PD MPS can be increased by increasing the operational parameters $Q_{mixing}$ or decreasing $V_{PD}$. However, exposure to unbound drug is also strongly modulated by the biological parameters *fu* and *P* (**Figure 5e**), over which we have little control. Exposure to total drug (bound plus unbound) follows similar trends, although the effect of *fu* is not nearly as strong as it is for unbound drug exposure (results not shown).

Another important drug characteristic is its rate of disappearance from the system. We characterized disappearance by calculating the percentage of total drug cleared in 48 hours after drug administration to the apical compartment of the gut. Unlike the parameters driving mixing above, sensitivity analysis showed that the most influential parameters driving percentage total drug cleared were related to drug elimination and bioavailability (**Supplementary Table 3**). As expected, increasing either metabolism or excretion increases system total drug cleared percentage, as shown in **Figure 5f** for $k_{metabolism,liver}$. $k_{excretion,kidney}$ has a similar effect since the flow rates of both liver and kidney MPS are similar (data not shown). Increasing *fu* also increases clearance since only the unbound drug is available to be metabolized or excreted (**Figure 5f**). Likewise, increasing gut permeability increases clearance since the drug must be absorbed through the intestinal epithelia of the gut MPS before it is cleared by MPSs.

Two parameters that strongly modulate system characteristics across all output metrics studied above are the mixing chamber outlet flowrate $Q_{mixing}$ and intestinal drug permeability coefficient *P*. Plotting drug concentration kinetics in the various MPSs as these parameters are varied provides additional insights and guidance for experimental design. **Figure 6** shows this for a drug bolus applied to the apical gut MPS at time = 0. As expected, drug concentration decreases as it moves from source (apical gut, **Figure 6**) to basal gut, liver, mixing chamber, and then all MPSs in parallel, according to the flow pattern in **Figure 4**. A high permeability drug transported with a high flowrate between MPSs (red lines) results in the highest drug exposure, highest maximum concentration ($C_{max}$), and earliest time to maximum ($t_{max}$) in the downstream MPSs, compared to either high *P*/low $Q_{mixing}$ (blue) or low *P*/high $Q_{mixing}$ (magenta) conditions (low *P*/low $Q_{mixing}$ results in even slower distribution between MPSs; not shown). Reducing $Q_{mixing}$ or *P* individually has different consequences in different MPSs: reducing $Q_{mixing}$ only (blue) results in drug accumulation in the basal gut, concentrations rising more slowly in the liver MPS and mixing chamber, and even more slowly in the kidney and the PD MPSs due to delays in reaching there as well as further dilution in additional media in those MPSs. In contrast, a low *P* drug with high $Q_{mixing}$ (magenta) has a low but relatively similar concentration profile everywhere, since the drug enters the system slowly but distributes quickly. Notably, reducing either $Q_{mixing}$ or *P* alone results in similar concentration profiles in the furthest downstream MPSs (kidney, PD).

The aggregate of all of these measures provides guidance to experimental design and operation: for a given set of MPS volumes, $t_{mixing,80}$ indicates when the system is close enough to uniform to sample from mixing chamber to approximate the PD MPS concentration; $AUC_{0\text{-}48}$ indicates whether exposure will be appropriate to elicit desired PD effects; percentage drug cleared at 48 hours indicates drug PK; and the kinetic profiles provide detailed dynamic information such as $C_{max}$ and $t_{max}$ in each MPS which can guide, for example, best sampling times.

## DISCUSSION

Single MPS and multi-MPS interactomes are sufficiently complex that the use of systems pharmacology models representing the many physical, chemical, and biological characteristics involved is crucial to MPS design, operation, and data interpretation. The challenge for systems pharmacology modeling is inclusion of enough mechanistic detail to capture key observable system behaviors without including so much that the models become unwieldy to simulate or interpret, or have so many parameters they cannot be constrained by measurable data. With these considerations in mind, we created a modeling framework to analyze data from our liver/immune MPS as well as to investigate operational principles for a hypothetical four-MPS interactome. Using this framework improves our understanding of biological and pharmacological processes in the MPSs and lays the groundwork for IVIVT.

We first demonstrated the use of our systems pharmacology framework to interpret experimental data from a single MPS, the liver/immune MPS, for two conditions: drug PK and disease response biomarkers. We demonstrated that adding mechanistic considerations to a traditional PK model could provide more detailed understanding of HC metabolism. Hence, we aimed to develop strategies for mechanistic data interpretation to obtain translational information from our experiments. Due to experimental restrictions, it is generally not feasible to mimic *in vivo* processes exactly and computational models are needed to translate *in vitro* data to *in vivo*. In the HC case study, our experimental setup had 47–95% unbound HC, whereas unbound HC in human plasma is around 7.5%.[27,37] Our mechanistic analysis showed that the unbound HC metabolism rate constant ($k_{metabolism,unbound}$) in the liver/immune MPS remained unchanged for different HSA concentrations. The mechanistic investigation of PK parameters, such as $k_{metabolism,unbound}$, could potentially be used for IVIVT. To predict *in vivo* pharmacokinetic properties of a given drug, proper scaling and translation need to be performed by considering several biological metrics (e.g., blood-to-tissue and media-to-tissue ratios, cell numbers, organ size, and plasma protein concentrations, etc.) for the MPSs and human physiology. Moreover, our systems pharmacology approach for data interpretation can be extended to more detailed models for in-depth understanding of pharmacology, which cannot be obtained by traditional PK models.

In our second liver/immune MPS case, we utilized a systems pharmacology model to interpret an inflammatory response to LPS stimulation. Because of the complex dynamics, a traditional PK/PD model would not capture, much less explain, the results. A more mechanistic model including ligand–receptor interactions and a minimal set of

receptor dynamics (internalization and recycling) was able to capture key observations, notably, differing kinetics of two response biomarkers, TNF-$\alpha$ and IL-6, as well as the lost response to a second high dose of LPS. Additional simulations were used to investigate the liver/immune MPS response to a range of LPS doses. The model predicts that studies of chronic inflammation will require an intermediate LPS dose that induces inflammation but does not cause saturation and extensive downregulation of TLR4 receptors. Next steps include experimental validation using a range of LPS doses, with modification of the model as needed. At that point the model will be well suited to guide design of inflammation studies in the liver/immune MPS (e.g., selection of inflammatory stimulus dose level and timing; appropriate times to sample response biomarkers; effects of modifying MPS design parameters).

A further interest is the use of multi-MPS platforms for pharmacological studies, which requires careful consideration of operational and biological parameters to attain desired distribution and exposure of exogenous and endogenous molecules in the various compartments. Although there are a few studies utilizing modeling and simulation for *in vitro* organ interaction studies,[38–40] no other study has used systems pharmacology models to comprehensively guide the design and operation of multi-MPS interactions. While the models in our single liver/immune MPS investigations included mechanistic detail for both drug PK and endogenous molecule production, we purposely eliminated the latter in this initial four-MPS study to make the results as general as possible. Such detail can be added for specific studies in the future.

Global sensitivity analysis along with examination of kinetic concentration profiles provides guidance on what drives important system outcomes. The practical utility of these analyses will be beneficial for the multi-MPS system developers and the experimental scientists and can best be understood through specific examples. First, consider studying the effects of a high permeability drug in the PD MPS following bolus administration to the apical side of the gut MPS ("oral administration"). Exposure to unbound drug in the PD MPS will be maximized by a high flowrate through the system (high $Q_{mixing}$) and increasing fraction of unbound drug in medium (high *fu*). A consequence of increasing *fu*, however, will be faster clearance by liver MPS and kidney MPS, so more frequent dosing may be needed. Selection of sampling times can be guided by the calculated $t_{mixing,80}$ for the specified operating conditions, along with the kinetic concentration profiles showing $C_{max}$ and $t_{max}$ in the PD MPS and other locations in the interactome.

A contrasting example is the same scenario for a low permeability drug. Now, high $Q_{mixing}$ has little effect on exposure in the PD MPS, and so exposure will be maximized only through use of a high *fu* or increasing the dose amount and/or frequency. High $Q_{mixing}$ will, however, drive a uniform distribution, allowing for easier interpretation of samples taken from the mixing chamber instead of a biological MPS, for example.

A third example is consideration of distribution of endogenously produced molecules through a multi-MPS interactome. For a given production rate, the concentration in the downstream MPS of the production location will be maximized by increased inter-MPS flowrate and reduced medium volume of the downstream MPS.

The selection of parameter values to use for any given experiment will require additional simulations that weigh the tradeoffs mentioned and selection of MPSs. Although our conclusions are strongly related to the multi-MPS schema considered, this study provides insights into approaches for experimental design and interactome operation.

In conclusion, the use of systems pharmacology models to analyze experimental results allows for a more mechanistic understanding of both the pharmacological and biological systems, which may lead to more predictive *in vitro–in vivo* translation. Furthermore, systems pharmacology models provided guidance for designing multi-MPS interactome studies in a quantitative manner. Both single MPSs and multi-MPS interactomes will greatly benefit from the use of quantitative, mechanistic models for their design, operation, data interpretation, and translation to humans.

**Acknowledgments.** Financial support for this project was provided by the DARPA Microphysiological Systems Program (W911NF-12-2-0039), the NIH Microphysiological Systems Program (4-UH3-TR000496-03), and MIT Center for Environmental Health Sciences (NIEHS Grant P30-ES002109).

**Author Contributions:** M.C., J.Y., N.C., and C.L.S. wrote the manuscript; M.C., J.Y., E.L., U.S., J.W., S.T., D.H., D.L., L.G., and C.L.S. designed the research; M.C., J.Y., E.L., U.S., and C.L.S. performed the research; M.C., J.Y., N.C., E.L., U.S., and C.L.S. analyzed the data; U.S. and J.W. contributed new reagents/analytical tools.

**Conflict of Interest:** The authors declare no conflicts of interests.

1. Arrowsmith, J. A decade of change. *Nat. Rev. Drug Discov.* **11**, 17–18 (2012).
2. Arrowsmith, J. & Miller, P. Trial watch: Phase II and Phase III attrition rates 2011-2012. *Nat. Rev. Drug Discov.* **12**, 569–569 (2013).
3. Hay, M., Thomas, D.W., Craighead, J.L., Economides, C. & Rosenthal, J. Clinical development success rates for investigational drugs. *Nat. Biotech.* **32**, 40–51 (2014).
4. Hartung, T. Toxicology for the twenty-first century. *Nature* **460**, 208–212 (2009).
5. Seok, J. *et al.* Genomic responses in mouse models poorly mimic human inflammatory diseases. *Proc. Natl. Acad. Sci. U. S. A.* **110**, 3507–3512 (2013).
6. Sorger, P.K. *et al.* Quantitative and systems pharmacology in the post-genomic era: new approaches to discovering drugs and understanding therapeutic mechanisms. An NIH white paper by the QSP workshop group 1–48 (NIH, Bethesda, MD, 2011).
7. Griffith, L.G. & Swartz, M.A. Capturing complex 3D tissue physiology in vitro. *Nat. Rev. Mol. Cell. Biol.* **7**, 211–224 (2006).
8. Sweeney, L.M., Shuler, M.L., Babish, J.G. & Ghanem, A. A cell culture analogue of rodent physiology: Application to naphthalene toxicology. *Toxicol. In Vitro* **9**, 307–316 (1995).
9. Sin, A., Baxter, G.T. & Shuler, M.L. Animal on a chip: A microscale cell culture analog device for evaluating toxicological and pharmacological profiles. *Proc. SPIE* **4560**, Microfluidics and BioMEMS 98 (2001). doi:10.1117/12.443045
10. Sin, A., Chin, K.C., Jamil, M.F., Kostov, Y., Rao, G. & Shuler, M.L. The design and fabrication of three-chamber microscale cell culture analog devices with integrated dissolved oxygen sensors. *Biotechnol. Prog.* **20**, 338–345 (2004).
11. Griffith, L.G. & Naughton, G. Tissue engineering–current challenges and expanding opportunities. *Science* **295**, 1009–1014 (2002).
12. Huh, D., Matthews, B.D., Mammoto, A., Montoya-Zavala, M., Hsin, H.Y. & Ingber, D.E. Reconstituting organ-level lung functions on a chip. *Science* **328**, 1662–1668 (2010).
13. Domansky, K., Inman, W., Serdy, J., Dash, A., Lim, M.H.M. & Griffith, L.G. Perfused multiwell plate for 3D liver tissue engineering. *Lab Chip* **10**, 51–58 (2010).

14. Yu, J., Peng, S., Luo, D. & March, J. In vitro 3D human small intestinal villous model for drug permeability determination. *Biotechnol. Bioeng.* **109**, 2173–2178 (2012).
15. Abaci, H.E., Gledhill, K., Guo, Z., Christiano, A.M. & Shuler, M.L. Pumpless microfluidic platform for drug testing on human skin equivalents. *Lab Chip* **15**, 882–888 (2015).
16. Gunther, A. *et al.* A microfluidic platform for probing small artery structure and function. *Lab Chip* **10**, 2341–2349 (2010).
17. Wang, Y., Ahmad, A.A., Sims, C.E., Magness, S.T. & Allbritton, N.L. In vitro generation of colonic epithelium from primary cells guided by microstructures. *Lab Chip* **14**, 1622–1631 (2014).
18. Lam, M.T., Huang, Y.-C., Birla, R.K. & Takayama, S. Microfeature guided skeletal muscle tissue engineering for highly organized 3-dimensional free-standing constructs. *Biomaterials* **30**, 1150–1155 (2009).
19. Fabre, K.M., Livingston, C. & Tagle, D.A. Organs-on-chips (microphysiological systems): tools to expedite efficacy and toxicity testing in human tissue. *Exp. Biol. Med.* **239**, 1073–1077 (2014).
20. Derendorf, H. & Meibohm, B. Modeling of pharmacokinetic/pharmacodynamic (PK/PD) relationships: concepts and perspectives. *Pharm. Res.* **16**, 176–185 (1999).
21. Csajka, C. & Verotta, D. Pharmacokinetic-pharmacodynamic modelling: history and perspectives. *J. Pharmacokinet. Pharmacodyn.* **33**, 227–279 (2006).
22. Ebrahimkhani, M.R., Neiman, J.A.S., Raredon, M.S.B., Hughes, D.J. & Griffith, L.G. Bioreactor technologies to support liver function in vitro. *Adv. Drug Del. Rev.* **69-70**, 132–157 (2014).
23. Vivares, A. *et al.* Morphological behaviour and metabolic capacity of cryopreserved human primary hepatocytes cultivated in a perfused multiwell device. *Xenobiotica* **45**, 29–44 (2015).
24. Clark, A.M. *et al.* A microphysiological system model of therapy for liver micrometastases. *Exp. Biol. Med.* **239**, 1170–1179 (2014).
25. Brown, R.P., Delp, M.D., Lindstedt, S.L., Rhomberg, L.R. & Beliles, R.P. Physiological parameter values for physiologically based pharmacokinetic models. *Toxicol. Ind. Health* **13**, 407–484 (1997).
26. Marino, S., Hogue, I.B., Ray, C.J. & Kirschner, D.E. A methodology for performing global uncertainty and sensitivity analysis in systems biology. *J Theor. Biol.* **254**, 178–196 (2008).
27. Gayrard, V., Alvinerie, M. & Toutain, P.L. Interspecies variations of corticosteroid-binding globulin parameters. *Domest. Anim. Endocrinol.* **13**, 35–45 (1996).
28. Rhen, T. & Cidlowski, J.A. Antiinflammatory action of glucocorticoids—new mechanisms for old drugs. *N. Engl. J. Med.* **353**, 1711–1723 (2005).
29. Slaunwhite, W.R., Lockie, G.N., Back, N. & Sandberg, A.A. Inactivity in vivo of transcortin-bound cortisol. *Science* **135**, 1062–1063 (1962).
30. Coolens, J.-L., Van Baelen, H. & Heyns, W. Clinical use of unbound plasma cortisol as calculated from total cortisol and corticosteroid-binding globulin. *J. Steroid Biochem.* **26**, 197–202 (1987).
31. Dorin, R.I. *et al.* Validation of a simple method of estimating plasma free cortisol: role of cortisol binding to albumin. *Clin. Biochem.* **42**, 64–71 (2009).
32. Mendel, C.M., Miller, M.B., Siiteri, P.K. & Murai, J.T. Rates of dissociation of steroid and thyroid hormones from human serum albumin. *J. Steroid Biochem. Mol. Biol.* **37**, 245–250 (1990).
33. Su, G.L. *et al.* Kupffer cell activation by lipopolysaccharide in rats: role for lipopolysaccharide binding protein and toll-like receptor 4. *Hepatology* **31**, 932–936 (2000).
34. Lu, Y.-C., Yeh, W.-C. & Ohashi, P.S. LPS/TLR4 signal transduction pathway. *Cytokine* **42**, 145–151 (2008).
35. Su, G.L. Lipopolysaccharides in liver injury: molecular mechanisms of Kupffer cell activation. *Am. J. Physiol. Gastrointest. Liver Physiol.* **283**, G256–G265 (2002). doi: 10.1152/ajpgi.00550.2001
36. Lin, W.-W. & Karin, M. A cytokine-mediated link between innate immunity, inflammation, and cancer. *J. Clin. Invest.* **117**, 1175–1183 (2007).
37. Poulin, P. & Theil, F.-P. Prediction of pharmacokinetics prior to in vivo studies. 1. Mechanism-based prediction of volume of distribution. *J. Pharm. Sci.* **91**, 129–156 (2002).
38. Sung, J.H., Kam, C. & Shuler, M.L. A microfluidic device for a pharmacokinetic-pharmacodynamic (PK-PD) model on a chip. *Lab Chip* **10**, 446–455 (2010).
39. Ghanem, A. & Shuler, M.L. Combining cell culture analogue reactor designs and PBPK models to probe mechanisms of naphthalene toxicity. *Biotechnol. Prog.* **16**, 334–345 (2000).
40. Tatosian, D.A. & Shuler, M.L. A novel system for evaluation of drug mixtures for potential efficacy in treating multidrug resistant cancers. *Biotechnol. Bioeng.* **103**, 187–198 (2009).



Supplementary information accompanies this paper on the *CPT: Pharmacometrics & Systems Pharmacology* website (http://www.wileyonlinelibrary.com/psp4)